Solution Kits for automated and robotic façade upgrading

K. Iturralde[a], P. Zimmermann[a], R.G.B. Santos[a], S. Das[a], W. Shen[a], M. Malik[a], S. Maio[a], A. Hidri[a], J. Shen[a], T. Bock[a]

[a] Chair of Building Realization and Robotics, School of Engineering and Design, Technical University of Munich, Germany
E-mail: kepa.iturralde@br2.ar.tum.de

Abstract –

In order to reach zero energy consumption of the current building stock, adding a new insulating envelope with Renewable Energy Sources onto the existing building is necessary. This can be achieved by using prefabricated modules, automation and robotics. Since the topic is complex, three main subcategories were defined: Data Flow, Off-site Manufacturing, and On-site Installation. Latest studies suggest that there are still gaps in the way of achieving economically feasible solutions. In other words, there must be a reduction in the working time achieved in each sub-category. In this paper four different solutions are explained: 1) online data processing of the building, 2) automated layout definition, 3) accurate measurement with targets and 4) Automated CAM generation and Manufacturing. The solutions are still being developed but the current results are promising.

Keywords –

Renovation; Prefabrication; Accuracy; Time

1 Introduction

One of the measures to cope with the Climate Change is by reducing globally the necessary amount of energy. Over recent years, strategies for achieving zero-energy consumption of buildings focused on insulating existing buildings and installing Renewable Energy Sources (RES) on top [1]. Applying this process manually implies two hazards: building user's intrusiveness and disturbances and risky activities carried out at heights. To avoid such inconveniences, prefabricated modules are manufactured off-site. These modules include insulation, RES, and other necessary components such as windows or waterproofing elements [2]. In previous research of automated, robotic façade renovation with prefabricated module aspects [3–5], three sub-categories were defined, as explained in Figure 1.

- SC1. Information or Data Flow. This section is related to the data acquisition of the existing building, the processing of the data and the definition of the prefabricated modules that are attached to the existing building. This information is used for the manufacturing of the modules, basically for creating a CAM (Computer Aided Manufacturing) for an off-site, manufacturing process. Besides, on-site, it is necessary to mark the location of the connectors on the existing wall.
- SC2. Off-site Manufacturing of the modules, which refers to the off-site automated manufacturing of the modules. Two phases can be differentiated; SC2.1, cut and machine the elements of the prefabricated modules, and SC2.2, assembly the module with the elements cut on previous point.
- SC3. On-site Installation of the modules. It deals with the process that spans from the arrival of the module to the site and the fixation of the modules to the existing building-wall. In robotic installation processes, the robot must be set up [6]. Apart from that, the connectors must be fixed and finally the modules need to be placed on top.

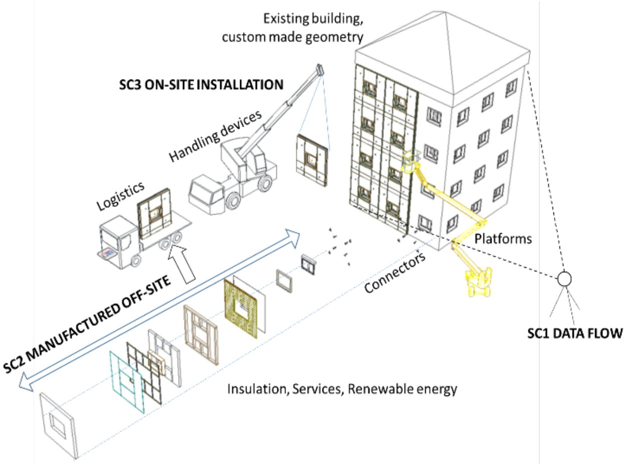

Figure 1. Scheme of the three sub-categories [6].

However, processes with prefabricated elements have not become competitive comparing to manual methods, which is the largest obstacle towards marketization. For this reason, a 90% reduction in data acquisition and processing was envisioned as one of the goals of the ENSNARE research project [7] where the research explained in this paper is based on. Shortening the current manufacturing and installation processes is an additional objective too.

However, working time reduction cannot come at the expense of losing quality, and regulation and standards must be fulfilled [8]. Data flow errors can lead to manufacturing modules with deviations. Minor deviations can lead to water and heat leaks, while larger deviations may cause collisions, or even jeopardize the installation of a module in its assigned location. Therefore, deviations of less than 2 mm are necessary to obtain an optimal result.

2 Research Gaps

Robotics and automated solutions in construction are only marketed when these are economically feasible [9–12]. The question of how to manage technology and make it ready for the market must also be addressed [13–15]. This topic has been approached in some different research projects such as BERTIM [16], and HEPHAESTUS [17]. In previous instances [18], up to 15 Research Gaps (RG) were detected. The research in this paper focuses on four RGs and their solutions. With respect to Data Flow, it was determined necessary to:

- RG1.1: Avoid recurrent data acquisition of the building. Online data for the initial measurements of the building should be explored, in order to avoid excessive visits to the existing building, especially on preliminary stages.
- RG1.2: Define automatically the layout definition of the modules. Normally, in building renovation, the preliminary definition of the module layout is defined manually, and it can take up to 15-20 hours in a low-rise building.
- RG1.3: Discriminate “unnecessary “information of the building, and determine the locations of the connectors using photogrammetry.

On the manufacturing process, the remaining RG considers how to:

- RG2: automate agile robot path adjustment depending on the layout-CAD of the modules. It is of a vital importance to generate a parametric adjustment of the robot path based on the CAD file of the module.

The remainder of this paper focuses on the developed solutions to these RGs.

3 Solution Kits

In order to improve the current process, a set of Solution Kits (SK) are being developed in the ENSNARE project. SK1 deals with online data acquisition, building definition, and online module layout definition. On the other hand, SK2 is related to the manufacturing process.

3.1 SK 1.1. Online data processing of the building

Online tools, such as *OpenStreetMaps*, were used for a preliminary semi-automated data acquisition and the subsequent initial building modelling. For that purpose, an algorithm was developed to generate semi-automatically the shape of the building (see Figure 2). Computational design tools and software, such as *FreeCAD* [19] were used to merge information taken from online databases.

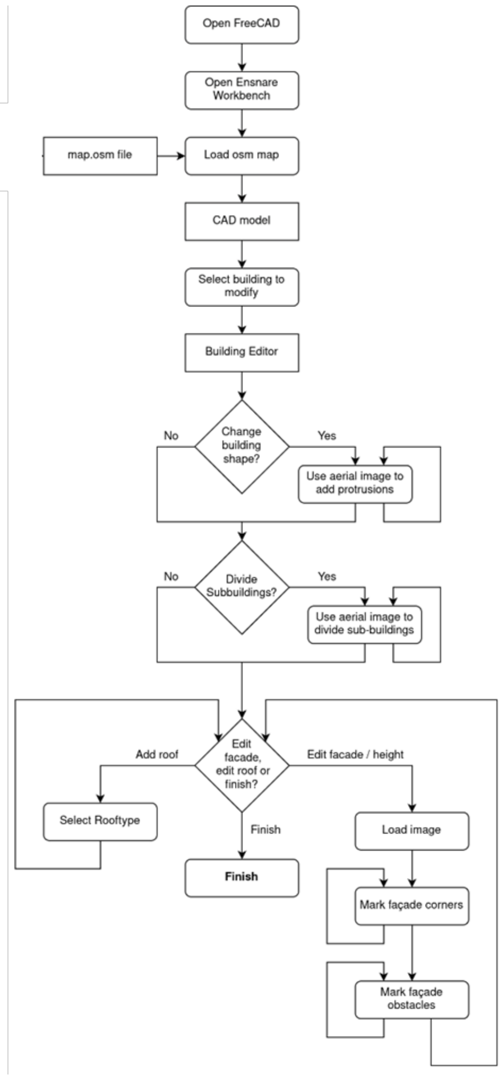

Figure 2. Scheme of the online data processing.

First, the user exports a map section from *OpenStreetMaps* as an *XML* file. The user then opens *FreeCAD* and uses the Load *.osm* file command to select the exported map file. The command creates a CAD object for each building in the OSM file with the correct layout (Figure 3). However, at this point the height of the building and the roof shape are unknown and height is estimated from the number of floors.

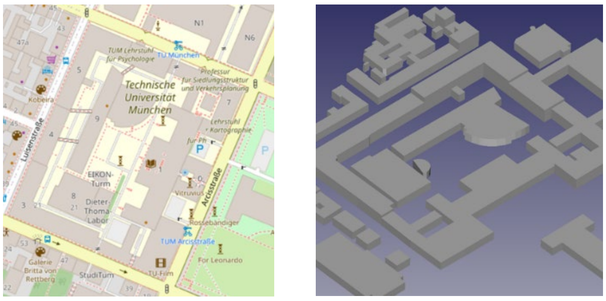

Figure 3. A map section in *OpenStreetMaps* (left) and the same map section after import in *FreeCAD* as 3D model (right).

In step two, the user selects a façade in the 3D view and uses the *Adjust façade* command. The user then selects a previously taken photo of the façade which is opened in a new window. In this window the corners of the façade can be marked by the user. With the corners given and by assuming a rectangular façade, we are able to locate the vanishing points. Through a series of geometrical operations, we are then able to revert the projection of the façade and determine the original proportion between width and height. Since the length of the façade is known from the *OpenStreetMaps* data we can multiply it with the proportion to calculate the building height. The height is then adjusted in the 3D model (see Figure 4).

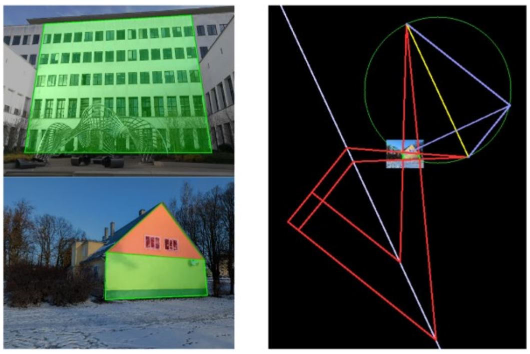

Figure 4. Left, façade photos with marked façade and gable area. Right, the algorithm for computing the height-width proportion from a façade image.

In step three, a perspective transformation is performed on the façade area to make it rectangular. In this transformed façade image, the user draws bounding boxes around façade objects and selects the appropriate object type, for example door or window. A grid selection mode is available for marking many objects in one step since objects like windows are frequently positioned in a grid. When the user has marked all objects on the façade, they can finish the step and the objects are added to the 3D model (see Figure 5).

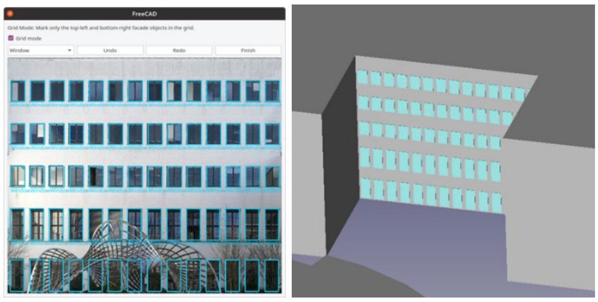

Figure 5. Marked windows with the grid function on transformed façade image.

When the user marks more than four corners for the façade, the additional points are interpreted as roof points. The roof shape is then extruded along the length of the building to create the roof in the 3D model (see Figure 6).

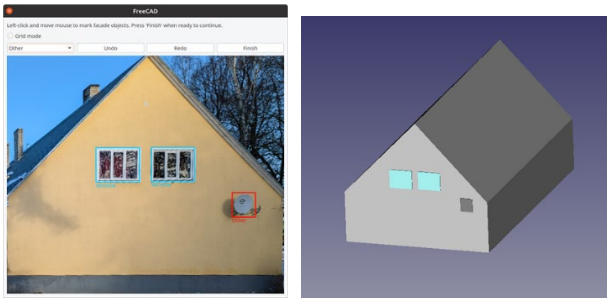

Figure 6. Different types of marked façade elements and pitched roof.

With the process described above, the building model can be defined. Several tests have been carried out, with satisfactory results, as shown in Figures 5 and 6. The difference between the obtained data and the actually measured building sizes ranges between 20 and 40 cm, depending on the size of the building. The differences are tolerable because SK1.1 is supposed to be used at the first stages of the façade renovation project. The measurements at this stage are used only for an estimation. With this building model, the layout of the modules can be determined automatically, as described in the next step.

3.2 SK1.2. Automated layout definition

The main focus of the prefabricated facade module model is that it is parametric. This means that a library of solutions can be used for various facade typologies and adjust accordingly. In order to have more flexibility, there are also criteria that the parameters must fulfill. These define the constraints of the model, such as:

- floor height of the given building
- window dimensions (if a window is present)
- vertical distance of the window from the floor
- solar panel dimensions

The foundations of the developed *FreeCAD* model are a sketch and a spreadsheet. In the sketch an abstracted two-dimensional drawing defines and visualizes the placement and size of the elements of a module. The desired placement and size is controlled through adjustable parameters, which in *FreeCAD* are addressed as constraints. Most of these constraints are defined in the spreadsheet. The rest are referenced in the sketch. Constraints (such as the height of the window) are first accessed through the spreadsheet, where they are given a value, then referenced with an alias, and finally linked in the constraints of the sketch in the form of a formula. This way of linking the data offers a parametric workflow. For modifying the constraints, it is only necessary to change the value of that constraint in the spreadsheet, and the model will adjust accordingly.

Regarding the solar panel's dimensions, several panel sizes are selected for this project. Their dimensions are listed in the spreadsheet. From case to case the right size of the solar panel for the module needs to be chosen; afterwards its dimensions need to be selected as values for the constraints.

The three-dimensional module model is comprised of several building elements belonging to the back frame and the panels on top. This is optimized for the later module assembly.

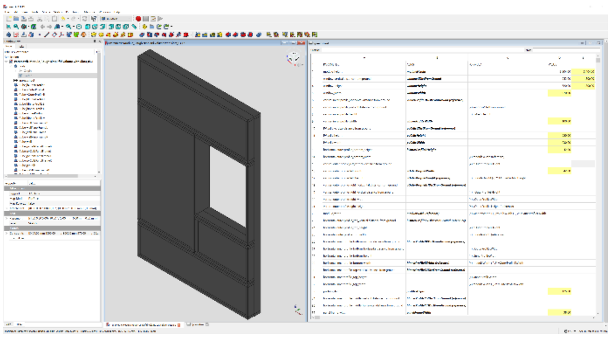

Figure 7. Different types of marked façade elements and pitched roof.

Currently the scenario in which the facade symmetrically admits modules which are all geometrically equivalent to each other is being developed. In this scenario the problem simplifies to placing a solar panel and accompanying registration area within just one module since this will be used to reconstruct the rest of the facade. Tackling more complex facades is a future task.

It is necessary to abstract the facade, module, solar panel, registration, and window as 2D regions in the plane. Under this abstraction the placement of the solar panel and registration area is a packing problem with the additional goal of maximizing the area of placed solar panel.

A module is represented as a rectangular region in the plane whose lower left vertex is at the origin as shown in Figure 8. The other features (the window, the solar panel, and the registration area) are rectangular regions subjected to the following constraints:

- A feature must be contained within the module.
- No two features may overlap.
- The registration area and solar panel must maintain some proximity.
- The registration area must be placed in a way that it can be reached by a neighboring module.

The approach is a greedy method that finds the first feasible configuration for a given solar panel. To ensure maximal surface area the approach starts with the solar panel of maximal area, and then moves on to the solar panel of second maximal area, and so on until all possible solar panels have been exhausted.

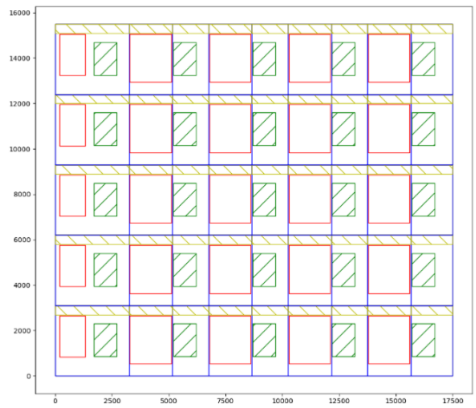

Figure 8. Automated maximization of the solar panels (red) and sub-division of the modules.

The implementation of the approach is done using python (version 3.6.9) without any external libraries. The solution is found by the function *find_optimal_placement* which takes the following inputs:

- the length, and height of the module
- the local coordinates of the bottom left corner of the window, its length, and its height
- a list of dimensions of potential solar panel
- a list of dimensions of possible registration areas
- a margin that specifies distance between features,

and distance features and the boundary of the module
- a step size which controls how many configurations are tested.

With the definition of the building module in SK1.1 and module layout definition described in this SK 1.2, the information is determined with high tolerances (see Figure 9).

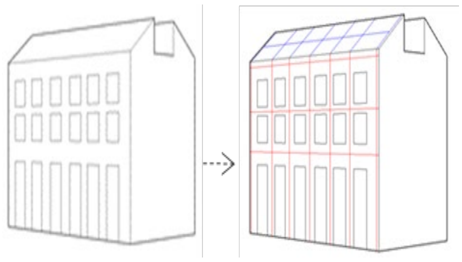

Figure 9. Automated generation of the layout.

The next section SK1.3 is based on the on-site accurate data acquisition of the building.

3.3 SK1.3. Accurate measurement with targets

In solution SK1.3, the so-called Matching Kit [20] is being redeveloped and improved. The Matching Kit consists of using the effectively measurement, markers, and using customized interfaces for adapting to existing buildings geometry. It has three main parts.
Part1 consists of targets that are placed on the existing building and gives information not only on the location, but also on the inclination of the wall. The Part1s will be placed on the existing building according to the preliminary layout developed in SK1.2 with an accuracy of 20 mm.

Part2 is located onto the prefabricated module depending on the location of Part1. In between both parts, an interface is placed which corrects the possible deviation of Part1 in regard to the planned position.

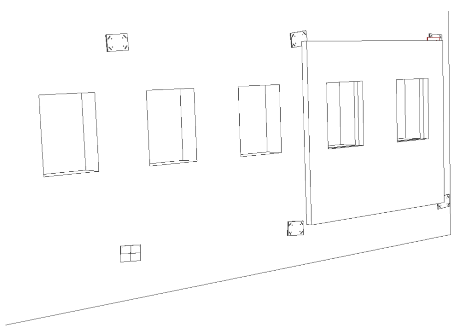

Figure 10. Part1s (markers) and the prefabricated modules.

The objective is to place and measure the markers in less than 8 hours for a low-rise building. In previous instances, Part1 was placed manually. In the project ENSNARE, a solution is being developed to place the Part1s by using drones, as shown in Figure 11.

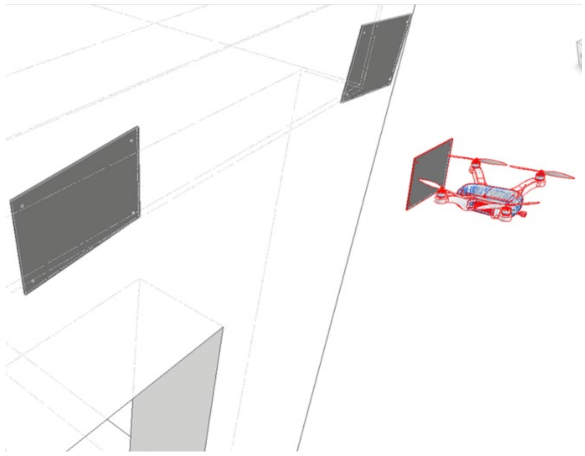

Figure 11. Placement of targets with drones.

In order to obtain the exact locations and angles of the Part1s, *AprilTag* markers are used and these are measured with photogrammetry methods. The 3D coordinates of the targets are estimated by an algorithm, with which the location and direction of each Part1 are obtained. Our goal is to measure the exact position and angle of each marker, and the error of the marker should not exceed 1mm at a distance of about 10m away from the building.

The following shows the entire process:

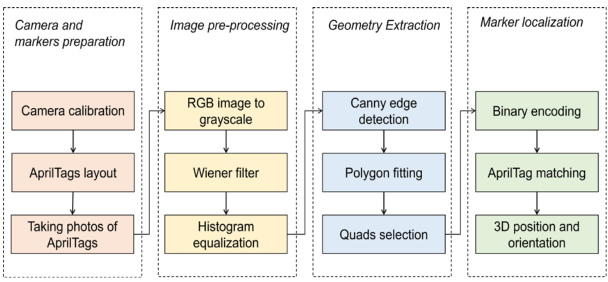

Figure 12. Scheme of the Part1s detection.

Before the measurement, the calibration of the camera is required. Zhang's calibration method [21] and Matlab's Camera Calibrator application to calibrate the camera [22] were used. Firstly, several photos of a 10 by 7 chessboard are taken by a digital camera from different angles. Then, those photos are imported into the calibrator, and after computing, the focal length, principal points, and distortion of the camera as a calibration matrix are determined. Next is the target localization. *AprilTag* is a visual targeting system that is useful for various tasks, including augmented reality, robotics, and camera calibration. Targets can be created with a common printer, and the *AprilTag* detection algorithm calculates the precise 3D position, orientation, and identity of the tag relative to the camera [23]. The detection algorithm has following steps: the color photos with targets are converted to grayscale, then the noises is reduced by an adaptive low-pass Wiener filter [24]. To make sure that the images are not too bright or too dark, the contrast using histogram equalization is enhanced. After that, we use the Canny edge detection algorithm to get the edges [25], fit the resulting edges into several closed polygons, and filter out the unqualified polygons, leaving only the quads. The candidate quads are binary encoded and if they match successfully with the *AprilTag* library, their IDs and the pixel positions of the 4 corners can be output.

Finally, we use PNP (perspective-n-point) method to solve the 3D position and orientation of each marker according to the 4 corners, marker size, and the camera calibration matrix.

With the information obtained in SK1.3, the data from SK1.2 is adjusted to a more accurate building description and therefore, low tolerance manufacturing can be achieved as explained on the next section SK2.

1.1 SK2: Automated CAM generation and Manufacturing

Once the data is processed and the prefabricated modules are defined as described in SK1.2 and SK1.3, this information is transformed to the robotic workstation that is used for producing and assembling modules. The idea behind it is to adjust the robot's path to the different geometry of each module.

As explained before, the geometry of the prefabricated modules varies, all are different. For this reason, for each of the prefabricated modules, a specific file layout information is used to define the coordinates of picking and placing of the robot.

First, for the CAM generation, a workbench named *viz. ENSNARE_CAD_CAM* was created. In this workbench, properties (placement and center of mass) of individual profiles of an entire module can be transported as a single *json* file.

The *FreeCAD* simulation window is shown in Figure 13 when some of the profiles of the module have been selected.

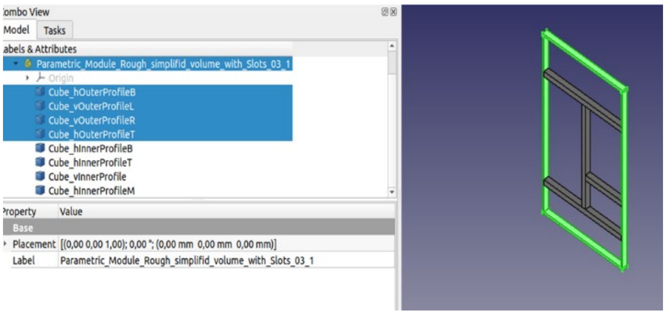

Figure 13. *FreeCAD* simulation.

Then, a Robot Operating System (ROS [26]) workspace was created which serves the purpose of providing the sequence of assembly of the profiles and the placement of individual profiles.

The process of retrieving the assembly is an automated process, which involves applying a simple nearest neighbor algorithm to select the next profile to be assembled. Once the sequence in which the profiles need to assembled is known from the previous service, the placement, i.e. the position, orientation and the center of mass of individual profiles is obtained through this service.

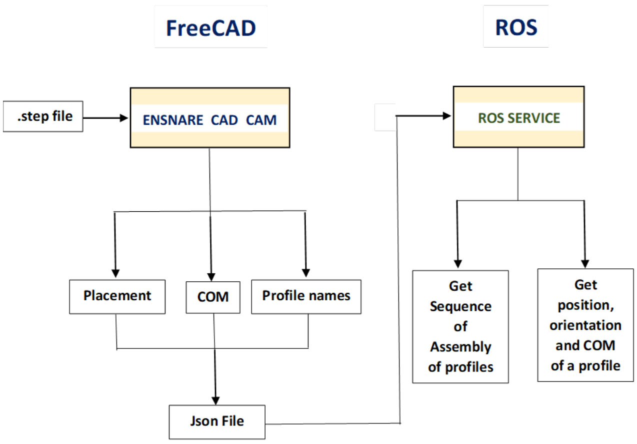

Figure 14. CAD-CAM synchronization scheme.

The robotic system mainly consists of a robotic arm (Universal Robot UR10e [27]) and a linear axis system. The base of the robotic arm is attached to the linear axis system which extends the reachability of the robotic arm. The linear axis system uses a stepper motor in combination with a gearbox to have enough torque to move the manipulator.

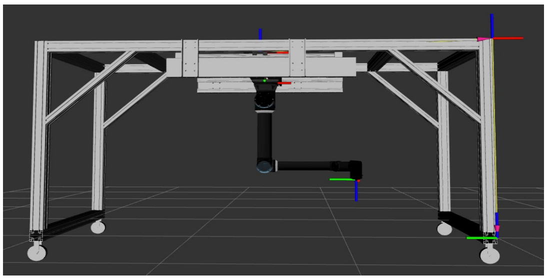

Figure 15. ROS simulation.

A Beckhoff PLC (Programmable Logic Controller) [28] is connected to the motor and offers an integrated position controller. Additionally, some sensors are used to define the limits of the linear axis. The below shows the configuration of the system.

The trajectory of the robotic arm and the pick and place operations are planned and executed by the motion planner *MoveIt* in ROS, which also includes collision checking. While the control of the manipulator is achieved by *MoveIt*, the motor in the rail system is controlled with a Beckhoff PLC. To synchronize the motion of both parts, a communication interface is created, where motion commands can be sent from a ROS node to the PLC machine, and the feedback position of the motor can be fetched from the PLC for a more accurate planning in *MoveIt*. The following Figure 16 shows the control scheme of the system.

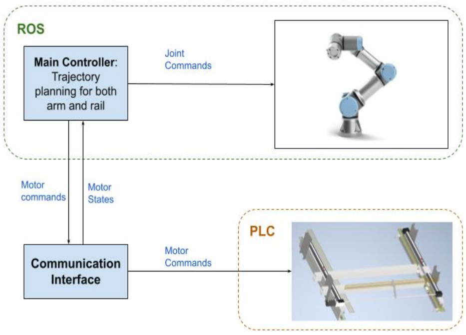

Figure 16. Control system of the robotic workstation

4 Conclusion

In this paper, a set of solutions for the automation of the façade renovation process have been explained. The solutions described in this paper are being developed currently. However, SK1.1 is almost finished and the building model can be generated by using online tools. This is a remarkable advance regarding building renovation with prefabricated models. The rest of the SKs, such as the robotic workstation in SK2 in Figure 17 still need more development and experimentations.

Moreover, the research gaps defined in [18] still need further revision and update.

Figure 17. Robotic workstation.

However, it must be remarked that if the solutions are developed as planned, close to market technology will be ready.

Acknowledgements

This project has received funding from the European Union's Horizon 2020 research and innovation programme under grant agreement No. 958445.

References

[1] Garay Martinez, R., Astudillo Larraz, J., Performance assessment of façade integrated glazed air solar thermal collectors, Energy Procedia. (2017) pp 353–360.

[2] Barco-Santa, A.F., Vareilles, É., Gaborit, P., Aldanondo, M., Building renovation adopts mass customization: {Configuring} insulating envelopes, Journal of Intelligent Information Systems. (2017) pp 119–146.

[3] Tsai, I.C., Kim, Y., Seike, T., Decision-making consideration in energy-conservation retrofitting strategy for the opening of existing building in Taiwan, AIJ J. Technol. Des. (2017). https://doi.org/http://doi.org/10.3130/aijt.23.963.

[4] Du, H., Huang, P., Jones, P.J., Modular facade retrofit with renewable energy technologies: the definition and current status in Europe, Energy and Buildings (205). (2019). https://doi.org/https://doi.org/10.1016/j.enbuild.2019.109543.

[5] D'Oca, S., Ferrante, A., Ferrer, C., Pernetti, R., Gralka, A., Sebastian, R., Op't Veld, P., Technical, financial, and social barriers and challenges in deep building renovation: Integration of lessons learned from the H2020 cluster projects, Buildings, 8. (2018) pp 174.

https://doi.org/https://doi.org/10.3390/buildings8120174.
[6] Iturralde, K., Study on Automated and Robotic Renovation of Building Façades with Prefabricated Modules, Technical University of Munich, 2021.
[7] ENSNARE Consortium, No Title, (2021). https://www.ensnare.eu/ (accessed July 27, 2021).
[8] DIN 18202 Toleranzen im Hochbau–Bauwerke, 2013.
[9] Skibniewski, M., Hendrickson, C., Analysis of Robotic Surface Finishing Work on Construction Site, Journal of Construction Engineering and Management. 114 (1988).
[10] Balaguer, C., Abderrahim, M., Trends in robotics and automation in construction., in: Intechopen, 2008. https://doi.org/10.5772/5865.
[11] Warszawski, A., Economic implications of robotics in building, Building and Environment. 20(2) (1985) pp 73–81. https://doi.org/https://doi.org/10.1016/0360-1323(85)90001-0.
[12] Hu, R., Iturralde, K., Linner, T., Zhao, C., Pan, W., Pracucci, A., Bock, T., A Simple Framework for the Cost–Benefit Analysis of Single-Task Construction Robots Based on a Case Study of a Cable-Driven Facade Installation Robot, Buildings. 11 (2021) pp 1–8. https://doi.org/10.3390/buildings11010008.
[13] Pan, M., Linner, T., Pan, W., Cheng, H., Bock, T., Structuring the context for construction robot development through integrated scenario approach., Automation in Construction. (2020). https://doi.org/https://doi.org/10.1016/j.autcon.2020.103174.
[14] Pan, M., Linner, T., Pan, W., Cheng, H., \& Bock, T., A framework of indicators for assessing construction automation and robotics in the sustainability context, Journal of Cleaner Production, 182. (2018) pp 82–95. https://doi.org/https://doi.org/10.1016/j.jclepro.2018.02.053.
[15] Pan, M., Linner, T., Pan, W., Cheng, H.M., Bock, T., Influencing factors of the future utilisation of construction robots for buildings: A Hong Kong perspective, Journal of Building Engineering. (2020). https://doi.org/https://doi.org/10.1016/j.jobe.2020.101220.
[16] BERTIM, D2.5. Efficient mass manufacturing and installation of prefabricated modules, 2016.
[17] Hephaestus_Consortium, Hephaestus - EU H2020 Project, (2017). https://www.hephaestus-project.eu/ (accessed October 5, 2021).
[18] Iturralde, K., Gambao, E., Bock, T., Compilation and assessment of automated façade renovation, in: Proceedings of the 38th International Symposium on Automation and Robotics in Construction (ISARC), Dubai, UAE, 2021: pp. 797–804. https://doi.org/10.22260/ISARC2021/0108.
[19] The FreeCAD Team, FreeCAD Your own 3D parametric modeler, (n.d.). https://www.freecadweb.org/.
[20] Iturralde, K., Linner, T., Bock, T., Matching kit interface for building refurbishment processes with 2D modules, Automation in Construction, 110. (2020). https://doi.org/https://doi.org/10.1016/j.autcon.2019.103003.
[21] Zhang, Z., A flexible new technique for camera calibration, IEEE Transactions on Pattern Analysis and Machine Intelligence. 22 (2000) pp 1330–1334. https://doi.org/10.1109/34.888718.
[22] Bouguet, J.Y., Camera Calibration Toolbox for Matlab, (n.d.). http://www.vision.caltech.edu/bouguetj/calib_doc/.
[23] Olson, E., AprilTag: A robust and flexible visual fiducial system, in: 2011 IEEE International Conference on Robotics and Automation, 2011: pp. 3400–3407. https://doi.org/10.1109/ICRA.2011.5979561.
[24] Treitel, S., THE COMPLEX WIENER FILTER, GEOPHYSICS. 39 (1974) pp 169–173. https://doi.org/10.1190/1.1440419.
[25] Rong, W., Li, Z., Zhang, W., Sun, L., An improved Canny edge detection algorithm, in: 2014 IEEE International Conference on Mechatronics and Automation, 2014: pp. 577–582. https://doi.org/10.1109/ICMA.2014.6885761.
[26] Robot Operating System, Robot Operating System Homepage, (2021). https://www.ros.org/ (accessed October 5, 2021).
[27] Universal Robots, UR10, (2021). https://www.universal-robots.com/products/ur10-robot/ (accessed September 30, 2021).
[28] Beckhoff, TwinCAT 3, (2021). https://www.beckhoff.com/en-en/products/automation/twincat/ (accessed October 5, 2021).